

## Magnetorotational Supernovae With Jets

G. S. Bisnovatyi-Kogan<sup>1,2</sup> \* and S. G. Moiseenko<sup>1</sup>

<sup>1</sup> Space Research Institute Rus. Acad. Sci, Moscow, Russia

<sup>2</sup> Joint Inst. Nuclear Research, Dubna, Russia

**Abstract** Core-collapse supernovae are accompanied by formation of neutron stars. The gravitation energy is transformed into the energy of the explosion, observed as SN II, SN Ib,c type supernovae. We present results of 2-D MHD simulations, where the source of energy is rotation, and magnetic field serves as a “transition belt” for the transformation of the rotation energy into the energy of the explosion. The toroidal part of the magnetic energy initially grows linearly with time due to differential rotation. When the twisted toroidal component strongly exceeds the poloidal field, magneto-rotational instability (MRI) develops, leading to a drastic acceleration in the growth of magnetic energy. Finally, a MHD shock wave is formed, producing a supernova explosion. Toy model of MRI development is presented. Mildly collimated jet is produced for dipole-like type of the initial field. Magnetorotational explosion may produce mirror asymmetric ejection, visible in the form of asymmetric jet, and formation of rapidly moving neutron stars - pulsars. Observational data on radio pulsars are discussed, which are well interpreted in this model.

**Key words:** supernovae – jets – magnetic field

### 1 INTRODUCTION

Supernova is one of the most powerful explosion in the Universe, energy release, radiation and kinetic, is about  $10^{51}$  erg. SNe explode at the end of evolution of massive stars, with initial mass more than  $\sim 8 M_{\odot}$ . Tracks in HR diagram for stars of different masses, up to white dwarf formation, or SN explosion, may be found in the review (Iben 1985). A thermonuclear explosion of C-O degenerate core with total disruption of the star take place in SN Ia. In a core collapse and formation of a neutron star, gravitational energy release  $\sim 6 \times 10^{53}$  erg, is carried away by neutrino (SN II, SN Ib,c) (Baade & Zwicky 1934). First numerical simulations of core-collapse SN had been performed by Colgate & White (1966).

### 2 MAGNETOROTATIONAL MECHANISM OF EXPLOSION.

There is a problem of transformation of the energy of weekly interacting neutrino into the kinetic one. Discovery of pulsars in 1968 year had shown, that neutron stars are rapidly rotating and strongly magnetized. In magnetorotational explosion (MRE) the transformation of the rotational energy of the neutron star into explosion energy takes place by means of the magnetic field (Bisnovatyi-Kogan 1970). Most supernova remnants are not spherically symmetrical. Neutron stars are rotating, and have magnetic fields up to  $10^{13}$  Gs, and even more. Often one-side ejections are visible. That indicate to non-spherical form of the SNe explosions. In differential rotating new born neutron stars radial magnetic field is twisted, and magnetic pressure becomes very high, producing MHD shock, by which the rotational energy is transformed to the explosion energy.

Calculations of MRE have been done by Bisnovatyi-Kogan et al. (1976), using the one-dimensional nonstationary equations of magnetic hydrodynamics, for the case of cylindrical symmetry. The energy

---

\* E-mail: [gkogan@iki.rssi.ru](mailto:gkogan@iki.rssi.ru)

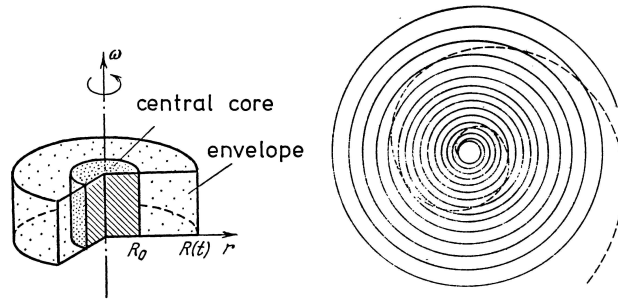


**Fig. 1** **Left:** A schematic picture of the initial state for the unit length of the cylinder (Bisnovatyi-Kogan et al. 1976). **Right:** Shape of the field lines in the region near the core at the time  $t = 7/\sqrt{\alpha}$ , for  $\alpha = 0.01$  (dashed line), and  $\alpha = 10^{-4}$  (solid line) (Ardeljan et al. 1979).

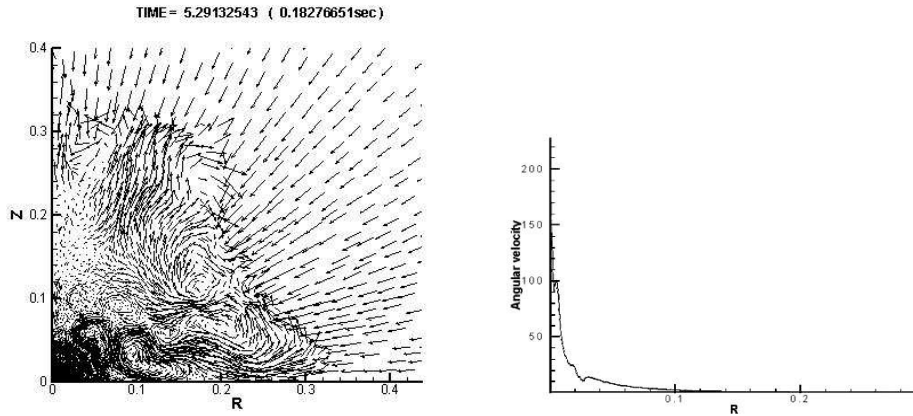


**Fig. 2** **left:** Velocity field, showing mixing of matter behind the shock at  $t = 0.1828$  (Ardeljan et al. 2004). **right:** Angular velocity distribution in the equatorial plane of the new born neutron star at  $t = 0.261$  after the beginning of the collapse.

source is supposed to be the rotational energy of the system (the neutron star, and surrounding envelope). The calculations show that the envelope splits up during the dynamical evolution of the system, the main part of the envelope joins the neutron star and becomes uniformly rotating with it, and the outer part of the envelope expands with large velocity, carrying out a considerable part of rotational energy and rotational momentum (Fig. 1). The main results of 1-D calculations are. MRE has an efficiency about 10% of the rotational energy. The ejected mass is  $\approx 0.1$  of the star mass, explosion energy  $\approx 10^{51}$  erg. Ejected mass and explosion energy depend very weakly on the parameter  $\alpha = E_{\text{mag}}/E_{\text{grav}}$  at initial moment. Explosion time depends on  $\alpha$  as  $t_{\text{expl}} \sim \frac{1}{\sqrt{\alpha}}$ . Small  $\alpha$  is difficult for numerical calculations with explicit numerical schemes because of the Courant restriction on the time step, stiff system of equations, where  $\alpha$  determines a stiffness. In 2-D computations implicit schemes have been used.

### 3 2-D CALCULATIONS

First 2-D calculations of MHD collapse have been done in LeBlanc & Wilson (1970). Implicit difference scheme based on Lagrangian triangular grid with grid reconstruction was developed in (Ardeljan & Chernigovskii 1984; Ardeljan et al. 1996). The scheme is fully conservative, what includes conservation of mass, momentum and total energy, and correct transitions between different types of energies.

### 3.1 Presupernova Core Collapse

Collapse and formation of a rapidly and differentially rotating neutron star had been calculated in Ardeljan et al. (2004) in non-magnetized approximation. Equations of state take into account degeneracy of electrons and neutrons, relativity for the electrons, nuclear transitions and nuclear interactions. Temperature effects were taken into account approximately by the addition of the pressure of radiation and of an ideal gas. Neutrino losses and iron dissociation were taken into account in the energy equations. A cool white dwarf was considered at the stability limit with a mass equal to the Chandrasekhar limit. To obtain the collapse we increase the density at each point by 20% and switch on a uniform rotation.

The hydrodynamical equations with gravity for modeling the nonstationary processes in rotating gaseous bodies are:

$$\begin{aligned} \frac{d\mathbf{x}}{dt} = \mathbf{v}, \quad \frac{d\rho}{dt} + \rho\nabla \cdot \mathbf{v} = 0, \quad \rho \frac{d\mathbf{v}}{dt} = -\nabla(P) - \rho\nabla\Phi, \\ \rho \frac{d\varepsilon}{dt} + P\nabla \cdot \mathbf{v} + \rho F(\rho, T) = 0, \quad \Delta\Phi = 4\pi G\rho. \end{aligned} \quad (1)$$

Here the equation of state and the function of neutrino losses have been represented by following functions

$$P \equiv P(\rho, T) = P_0(\rho) + \rho\Re T + \frac{\sigma T^4}{3}, \quad \varepsilon = \varepsilon_0(\rho) + \frac{3}{2}\Re T + \frac{\sigma T^4}{\rho} + \varepsilon_{Fe}(\rho, T), \quad (2)$$

where  $\varepsilon_{Fe}(\rho, T)$  is the iron dissociation energy,  $F(\rho, T)$  is the function of neutrino losses, among which only the URCA process losses are important. Other losses, such as pair annihilation, photo production of neutrino, plasma neutrino were also included in the calculations.

$$P_0(\rho) = \begin{cases} P_0^{(1)} = b_1\rho^{1/3}/(1 + c_1\rho^{1/3}), & \rho \leq \rho_1, \\ P_0^{(k)} = a \cdot 10^{b_k(\lg\rho - 8.419)^{c_k}} & \rho_{k-1} \leq \rho \leq \rho_k, \quad k = \overline{2, 6}, \end{cases} \quad (3)$$

$$\varepsilon = \varepsilon_0(\rho) + \frac{3}{2}\Re T + \frac{\sigma T^4}{\rho} + \varepsilon_{Fe}(\rho, T), \quad \varepsilon_0(\rho) = \int_0^\rho \frac{P_0(\tilde{\rho})}{\tilde{\rho}^2} d\tilde{\rho}, \quad (4)$$

$$\varepsilon_{Fe}(\rho, T) = \frac{E_{b,Fe}}{A m_p} \left( \frac{T - T_{0Fe}}{T_{1Fe} - T_{0Fe}} \right).$$

$$f(\rho, T) = \frac{1.3 \cdot 10^9 \alpha(\bar{T}) \bar{T}^6}{1 + (7.1 \cdot 10^{-5} \rho / \bar{T}^3)^{2/5}} \text{ erg} \cdot \text{s}^{-1}, \quad \bar{T} = T \cdot 10^{-9}, \quad (5)$$

$$\alpha(\bar{T}) = \begin{cases} 1, & \bar{T} < 7, \\ 664.31 + 51.024(\bar{T} - 20), & 7 \leq \bar{T} \leq 20, \\ 664.31, & \bar{T} > 20, \end{cases} \quad (6)$$

The URCA losses  $f(\rho, T)$  have been described by formula in Bisnovaty-Kogan et al. (1976), obtained by approximation of tables from Ivanova et al. (1969). Other losses (unimportant) are included in  $Q_{\text{tot}}$ .

$$F(\rho, T) = (f(\rho, T) + Q_{\text{tot}}) e^{-\frac{\tau_\nu}{10}}. \quad (7)$$

Neutrino absorption is important in deeper layers of the neutron star. It is taken into account implicitly, by multiplying the transparent neutrino flux by the multiplayer  $e^{-\frac{\tau_\nu}{10}}$ , where the effective neutrino optical depth  $\tau_\nu$  is calculated using local density gradients (Ardeljan et al. 2004, 2005). Initial state was chosen as a spherically symmetric star, with a mass 20% larger than the limiting mass of the corresponding white dwarf  $M = 1.0042 M_\odot + 20\%$ , and rotating uniformly, with an angular velocity  $2.519 \text{ (sec}^{-1}\text{)}$ . The temperature distribution was taken in the form  $T = \delta\rho^{2/3}$ .

Results of calculations are represented in Figure 2. The collapse is stopped due to formation of a stable neutron core, rotating almost uniformly. The shock is reflected from the core, leaving behind a hot

plasma, where vortexes are generated. It leads to a strong mixing, what is important for the interpretation of observations of the light curve of SN 1987A. The light curve, corresponding to the radioactive decay of  $^{56}\text{Ni} \rightarrow ^{56}\text{Co} \rightarrow ^{56}\text{Fe}$  was observed in this object, what could be explained by enrichment of the outbursting matter due to mixing with deeper layers.

The main result of these calculations is a self-consistent model of the rapidly rotating neutron star with a differentially rotating envelope. The adjusting parameters are chosen to reproduce the calculations with a refined account of the neutrino transport (Burras et al. 2003). In correspondence with these calculations we have obtained that the bounce shock wave and neutrino deposition do not produce SN explosion. Distribution of the angular velocity is represented in Figure 2. The period of rotation of the almost uniformly rotating core of the young neutron star is about 0.001 s.

### 3.2 2-D Magnetorotational Supernova

Calculations of magnetorotational core-collapse supernova have been performed in (Ardeljan et al. 2005). Magnetohydrodynamic (MHD) equations with self-gravitation, and infinite conductivity have been solved using the same numerical scheme as described above. The set of equations is the following:

$$\begin{aligned} \frac{d\mathbf{x}}{dt} &= \mathbf{v}, & \frac{d\rho}{dt} + \rho \nabla \cdot \mathbf{v} &= 0, \\ \rho \frac{d\mathbf{v}}{dt} &= -\text{grad} \left( P + \frac{\mathbf{H} \cdot \mathbf{H}}{8\pi} \right) + \frac{\nabla \cdot (\mathbf{H} \otimes \mathbf{H})}{4\pi} - \rho \nabla \Phi, \\ \rho \frac{d}{dt} \left( \frac{\mathbf{H}}{\rho} \right) &= \mathbf{H} \cdot \nabla \mathbf{v}, & \Delta \Phi &= 4\pi G \rho, \\ \rho \frac{d\varepsilon}{dt} + P \nabla \cdot \mathbf{v} + \rho F(\rho, T) &= 0, & P &= P(\rho, T), \quad \varepsilon = \varepsilon(\rho, T), \end{aligned} \quad (8)$$

where  $\frac{d}{dt} = \frac{\partial}{\partial t} + \mathbf{v} \cdot \nabla$  is the total time derivative,  $\mathbf{x} = (r, \varphi, z)$ ,  $\mathbf{v} = (v_r, v_\varphi, v_z)$  is the velocity vector,  $\rho$  is the density,  $P$  is the pressure,  $\mathbf{H} = (H_r, H_\varphi, H_z)$  is the magnetic field vector,  $\Phi$  is the gravitational potential,  $\varepsilon$  is the internal energy,  $G$  is gravitational constant,  $\mathbf{H} \otimes \mathbf{H}$  is the tensor of rank 2, and  $F(\rho, T)$  is the rate of neutrino losses. Equation of state and the function of neutrino losses have been the same as in the previous section. Additional condition here is  $\nabla \cdot \mathbf{H} = 0$ . The problem has an axial symmetry ( $\frac{\partial}{\partial \phi} = 0$ ), and the symmetry to the equatorial plane ( $z=0$ ). Boundary conditions are the following:

$$\begin{aligned} P = \rho = T = B_\phi = 0 & \text{ at the outer boundary; } & v_r = j_r = B_r = 0 & \text{ at } r = 0; \\ v_\phi = j_\phi = B_\phi = 0 & \text{ at } r = 0; & v_z = 0, & \\ \frac{\partial B_z}{\partial z} = 0 & \text{ (dipole-like) or } B_z = 0 & \text{ (quadrupole-like) at } z = 0. \end{aligned} \quad (9)$$

Initial toroidal current  $J_\phi$  (see Fig. 3) was taken at the initial moment (time started now from the stationary rotating neutron star) producing  $H_r, H_z$  according to Bio-Savara law

$$\mathbf{H} = \frac{1}{c} \int_V \frac{\mathbf{J} \times \mathbf{R}}{R^3} dV, \quad (10)$$

Initial magnetic field of quadrupole-like symmetry is obtained at opposite directions of the current in both hemispheres (Fig. 3). Magnetic field is amplified due to twisting by the differential rotation, and subsequent development of the magnetorotational instability. The field distribution for initial quadrupole-like magnetic field with  $\alpha = 10^{-6}$ , at the moment of the maximal energy of the toroidal magnetic field is represented in Figure 4. Two dark areas: near the equatorial plane, and around the axis at  $45^\circ$ , show the regions with local maxima of the toroidal magnetic field  $H_\phi^2$ . The maximal value of  $H_\phi = 2.5 \times 10^{16}$  Gs was obtained in the calculations. The magnetic field at the surface of the neutron star after the explosion is  $H = 4 \times 10^{12}$  Gs

Time dependences during the explosion of different types of the energy: rotational energy, gravitational energy, internal energy, kinetic poloidal energy, are given in Figure 5. Almost all gravitational energy,

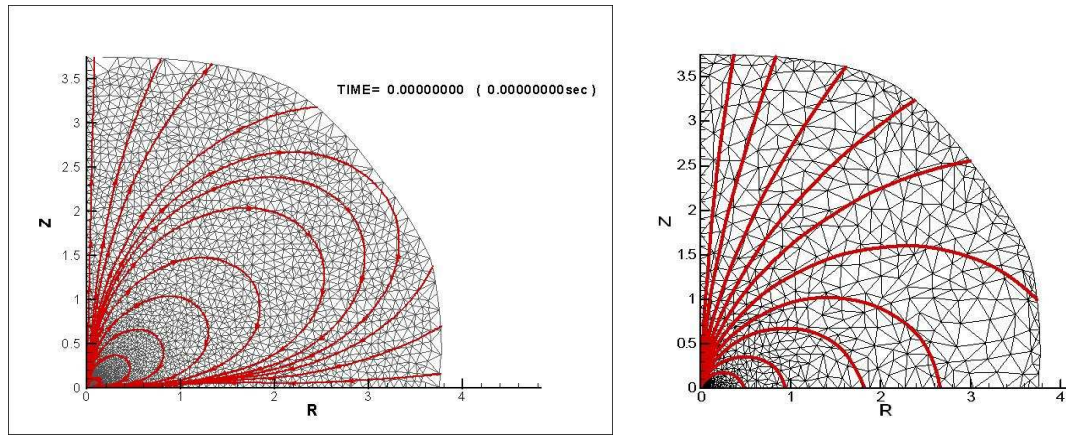


**Fig. 3** **left:** Initial quadrupole-like magnetic field, at  $t = 0$ . **right:** Initial dipole-like magnetic field, at  $t = 0$ .

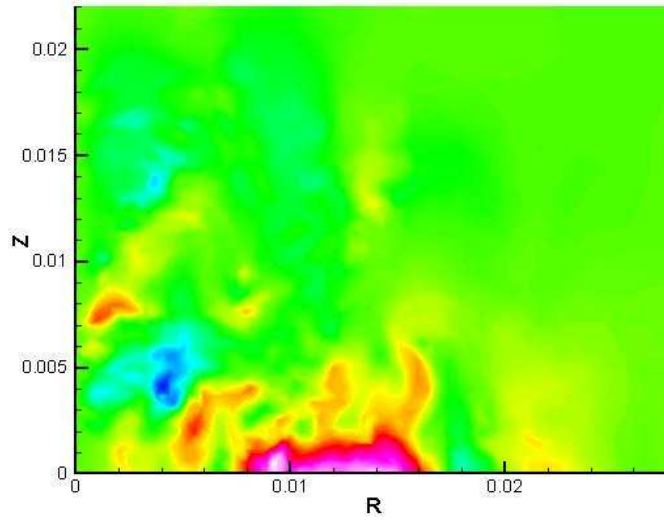


**Fig. 4** Toroidal magnetic field distribution at the moment of its maximal energy.

transforming into heat during the collapse, is carried away by weakly interacting neutrino. A mass “particle” is considered ejected if its kinetic energy is greater than its potential energy. The total energy ejected in the kinetic form is equal to  $0.6 \times 10^{51}$ , and the total ejected mass is equal to  $0.14 M_{\odot}$ .

#### 4 MAGNETOROTATIONAL INSTABILITY

Magnetorotational instability (MRI) leads to exponential growth of magnetic fields. Different types of MRI are have been studied in (Velikhov 1959; Spruit 2002; Akiyama et al. 2003). MRI starts to develop when the ratio of the toroidal to poloidal magnetic energies is becoming large. In 1-D calculations MRI is absent because of a restricted degree of freedom. Therefore the time of MR explosion is increasing with  $\alpha$  as  $t_{\text{expl}} \sim \frac{1}{\sqrt{\alpha}}$ ,  $\alpha = \frac{E_{\text{mag0}}}{E_{\text{grav0}}}$ . Due to development of MRI the time of MR explosion depends on  $\alpha$  much weaker. The ratio of two magnetic energies is changing with time almost with the same speed for all  $\alpha$ , so MRI starts almost at the same time. The MR explosion happens when the magnetic energy is becoming comparable to the internal energy, at least in some parts of the star. While the starting magnetic energy

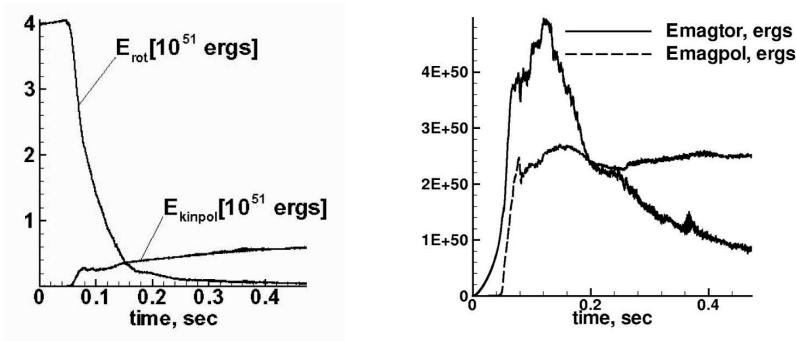


**Fig. 5** Time dependence of rotational, kinetic poloidal, and magnetic energies during explosion for a quadrupole-like field (from Ardeljan et al. 2005).

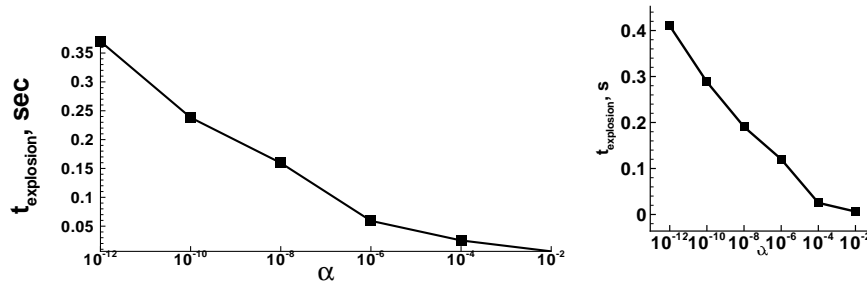


**Fig. 6** Duration of the explosion time on  $\alpha$  in presence of MRI for quadrupole (**left**), (from Ardeljan et al. 2005), and dipole (**right**) initial magnetic fields (from Moiseenko et al. 2006).

linearly depends on  $\alpha$ , and MRI leads to exponential growth of the magnetic energy, the total time of MRE in 2-D is growing **logarithmically**, see Figure 6, with decreasing of  $\alpha$ ,  $t_{\text{expl}} \sim -\log \alpha$ . This dependences are seen clearly from 1-D and 2-D calculations with different  $\alpha$  giving the following explosion times  $t_{\text{expl}}$  (in arbitrary units):

$$\begin{aligned} \alpha = 0.01, t_{\text{expl}} = 10, \quad \alpha = 10^{-12}, t_{\text{expl}} = 10^6 \quad \text{in 1-D}, \\ \alpha = 10^{-6}, t_{\text{expl}} \sim 6, \quad \alpha = 10^{-12}, t_{\text{expl}} \sim 12 \quad \text{in 2-D}. \end{aligned} \quad (11)$$

#### 4.1 Toy Model of the MRI Development

Toy model of the MRI development shows an exponential growth of the magnetic fields at initial stages of MRI development in 2-D. Initially MRI leads to formation of multiple poloidal differentially rotating vortices. Angular velocity of vortices is growing (linearly) with a growth of  $H_\phi$ .

$$\frac{dH_\phi}{dt} = H_r \left( r \frac{d\Omega}{dr} \right). \quad (12)$$

The right-hand side is constant at the initial stage of the process. When toroidal field reaches its critical value  $H_\phi^*$ , the MRI instability starts to develop. As follows from our calculations, the critical value corresponds to the ratio between total over the star toroidal and poloidal magnetic energies  $\sim 1 - 3$ . A local value of this critical ratio is much larger, reaching at the beginning of MRI  $\sim 10^4$  in the regions of the maximal growth of the toroidal magnetic field, what in time roughly corresponds to about 100 rotations of the neutron star core. These regions serve as germs for subsequent development of MRI in other parts of the star. The appearance

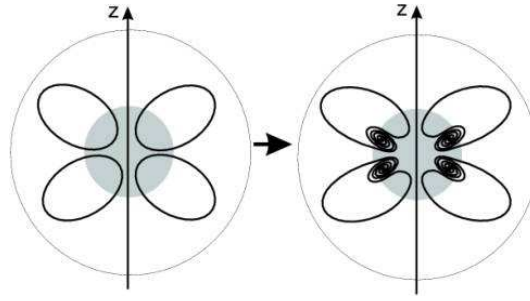


Fig. 7 Qualitative picture of the development of the MRI in 2-D.

of MRI is characterized by formation of multiple *poloidal* differentially rotating vortices, which twist the initial poloidal field leading to its amplification according to

$$\frac{dH_r}{dt} = H_{r0} \left( \frac{d\omega_v}{dl} l \right), \quad (13)$$

where  $l$  is the coordinate, directed along the vortex radius,  $\omega_v$  is the angular velocity of the poloidal vortex. Qualitatively the poloidal field amplification due to the vortices induced by MRI is shown in the Figure 7. The enhanced poloidal field immediately starts to take part in the toroidal field amplification according to Equation (12). With further growing of  $H_\varphi$  the poloidal vortex speed increases. Our calculations give the values of  $\omega_v = 0.0132 \text{ s}^{-1}$  at  $|H_\varphi| = 2.46 \times 10^{15} \text{ G}$  corresponding to  $t = 0.041 \text{ s}$  and  $\omega_v = 0.052 \text{ s}^{-1}$  at  $|H_\varphi| = 4.25 \times 10^{15} \text{ G}$  corresponding to  $t = 0.052 \text{ s}^{-1}$  for the same Lagrangian particle. In general we may approximate the value in Equation (13) by linear function on the value  $(H_\varphi - H_\varphi^*)$  as

$$\left( \frac{d\omega_v}{dl} l \right) = \alpha(H_\varphi - H_\varphi^*), \quad \frac{d^2}{dt^2} (H_\varphi - H_\varphi^*) = AH_{r0}\alpha(H_\varphi - H_\varphi^*), \quad (14)$$

$$H_\varphi = H_\varphi^* + H_{r0} e^{\sqrt{A\alpha H_{r0}}(t-t^*)}, \quad (15)$$

$$H_r = H_{r0} + \frac{H_{r0}^{3/2} \alpha^{1/2}}{\sqrt{A}} \left( e^{\sqrt{A\alpha H_{r0}}(t-t^*)} - 1 \right), \quad (16)$$

## 5 JET FORMATION IN MRE

Jet formation in MRE happens when the initial magnetic field is of a dipole-like structure (Fig. 3). 2-D calculations with the initial dipole-like magnetic field gave almost the same values of the energy of explosion  $\sim 0.5 \times 10^{51}$  and ejected mass  $\approx 0.14 M_\odot$ , but the outburst was slightly collimated along the rotational axis (Moiseenko et al. 2006), see Figure 8.

Large velocities observed in some radiopulsars, sometimes exceeding  $1000 \text{ km s}^{-1}$  Vlemmings et al. 2005, indicate to braking of a mirror symmetry during SN explosion. In a strong magnetic field, when there is a high level of polarization in the the electron distribution, asymmetric neutrino emission may be connected with CP violation in weak interactions (Chugai 1984). Our calculations, where rapid development of MRI is obtained, have shown that CP violation in week processes, where a regular magnetic field is needed, does not work, because MRI leads to formation of highly chaotic field configuration.

The models with a powerful neutrino convection, was considered by (Burrows at al. 1995; Janka & Müller 1995). They obtained a strong asymmetry of neutrino emission in a spherically symmetric collapse, with arbitrary direction of the kick velocity. Subsequent calculations (Dessart et al. 2006) have shown a minor role of neutrino convection: “Proto Neutron Star convection is thus found to be a secondary feature of the core-collapse phenomenon, rather than a decisive ingredient for a successful explosion”.

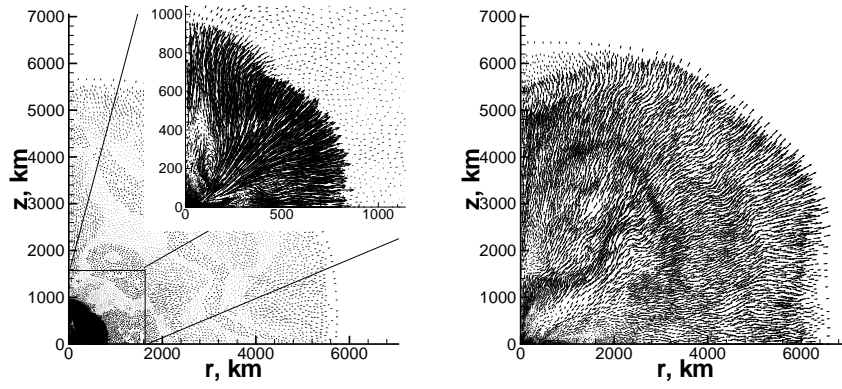


**Fig. 8** Time evolution of the velocity field for time moments  $t = 0.075s$  (left),  $t = 0.25s$  (right), from (Moiseenko et al. 2006).

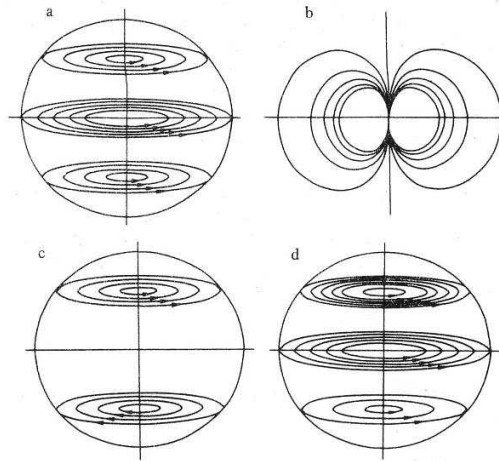


**Fig. 9** a) Initial toroidal field. b) Initial dipole field. c) Generated toroidal field. d) Resulted toroidal field.

In the paper (Bisnovatyi-Kogan & Moiseenko 1992) we have considered a violation of the mirror symmetry of the magnetic field in differentially rotating stars, when initial toroidal and poloidal fields have opposite symmetries. It happens when a star has a symmetric toroidal field with the dipole, or antisymmetric poloidal field with the quadrupole, see Figure 9. During the differential rotation initial poloidal field generate toroidal field of opposite symmetry. Combination of the initial and induced toroidal fields produce a toroidal field without the mirror symmetry. In magnetorotational supernova, the kick velocity along the rotational axis is expected due to the asymmetry of the magnetic field up to  $\sim 300 \text{ km s}^{-1}$  (Bisnovatyi-Kogan & Moiseenko 1992). Stronger kick is expected due to asymmetry of the neutrino emission in asymmetric magnetic field. It was obtained by O'Connell and Matese (1969), than neutron decay  $W_n$  probability increase linearly with  $B$  at  $B \gg B_c$ , where

$$B_c = \frac{m_e^2 c^3}{e \hbar} = 4.4 \times 10^{13} \text{ Gs}, \quad (17)$$

so that

$$W_n = W_0 [1 + 0.17(B/B_c)^2 + \dots] \text{ at } B \ll B_c, \quad W_n = 0.77W_0(B/B_c) \text{ at } B \gg B_c. \quad (18)$$

In relativistic degenerate electrons with fermi energy  $\beta = \varepsilon_F/m_e c^2 \gg 1$ , the critical magnetic field is  $\beta$  times larger. The dependence  $W_n(B)$  leads to anisotropic neutrino mean free path  $l_T$ , anisotropic neutrino opacity  $\kappa_\nu = 1/l_T \rho$ , and asymmetric neutrino flux on the level of neutrinosphere  $r_\nu$ . At large neutrino opacity neutrino heat flux  $H_\nu$  is connected with the temperature gradient, and may be written as (Imshennik & Nadjozhin 1972)

$$H_\nu = -\frac{7}{8} \frac{4acT^3}{3} l_T \frac{\partial T}{\partial r}, \quad (19)$$

and asymmetry of the neutrino flux may be estimated as (Bisnovaty-Kogan 1993)

$$\delta_L = \frac{L_+ - L_-}{L_+ + L_-}, \quad L = 4\pi r_\nu^2 H_\nu. \quad (20)$$

At a simplified approximation the formula for a kick velocity due to anisotropy of a neutrino flux was obtained in the form (Bisnovaty-Kogan 1993)

$$v_{nf} = \frac{2}{\pi} \frac{L_\nu}{M_n c} \frac{PB_{\phi 0}}{|B_p|} \left(0.5 + \ln \left( \frac{20 \text{ s } |B_p|}{P B_{\phi 0}} \right)\right). \quad (21)$$

For the value  $x = \frac{B_{\phi 0}}{|B_p|}$  between 20 and  $10^3$ , we have  $v_{nf}$  between 140 and 3000 km s<sup>-1</sup>. It is important, that in the case of an inclined rotator the asymmetry is developing along the rotational axis, and not the magnetic one (Hanawa et al. 2006), so the kick velocity should be directed along the rotational axis in this model. The correlation between the directions of the kick velocity and axis of rotation was found in (Johnston et al. 2005) by analysis of a large sample of radiopulsars.

In reality we have dipole, quadrupole, and other multipoles all together. Therefore the magnetic field may be asymmetric from the very beginning (Wang et al. 1992). A good example is the large scale solar magnetic field, which has the north-south coronal asymmetry with inferred magnetic quadrupole (Osherovich et al. 1999).

## 6 DISCUSSION

The results of the 2D numerical simulations of the MR supernova explosion with the initial dipole-like magnetic field have shown that MR supernova explosion is sensitive to the magnetic field configuration. MR supernova explosion with the initial quadrupole-like magnetic field develops mainly near the equatorial plane. In the case of the dipole-like magnetic significant part of the ejected matter obtains a velocity along the rotational axis. The total energy of the explosion in the MR mechanism does not depend significantly on the topology of the initial magnetic field. The explosion energy for quadrupole-like and dipole-like magnetic fields are similar,  $\sim 0.61 \times 10^{51}$  erg, and  $\sim 0.5 \times 10^{51}$  erg respectively. The amount of the ejected mass is approximately the same in both cases  $M_{\text{ejected}} \approx 0.14 M_\odot$ . Comparison of the explosion times for the dipole-like and the quadrupole-like fields of the same initial magnetic energy, shows that in the quadrupole case the explosion is developing faster. The time of the explosion for the  $\alpha = 10^{-6}$  is about  $\sim 0.12$  s in the dipole case, and is about  $\sim 0.06$  s in the case of the quadrupole.

In both cases we have done 2D simulations in a wide range of the initial magnetic field strength. The parameter  $\alpha$  (the ratio between the initial magnetic energy and the gravitational energy of the star at the moment of “turning on” of the magnetic field) was chosen as

$$\alpha = \frac{E_{\text{mag}0}}{|E_{\text{gr}}|} = 10^{-2} \div 10^{-12}. \quad (22)$$

Comparison of the results of 1D simulations from (Ardeljan et al. 1979), with a dependence of the MR explosion time on  $\alpha$  as  $t_{\text{expl}} \sim \frac{1}{\sqrt{\alpha}}$ , with corresponding 2D results (Fig. 6), shows a qualitative difference between them. The reason is a development of the MRI in 2D-case, which reduces drastically the MR explosion time  $t_{\text{expl}}$ . For the values of  $\alpha > \sim 10^{-4}$  the inverse square dependence holds approximately, while for smaller  $\alpha$  values the MR explosion time depends on  $\alpha$  as  $t_{\text{expl}} \sim |\log \alpha|$ . The axial protojet forming in our simulations is not narrow, while propagating through the envelope of the massive star this protojet could be collimated.

In the paper by Sawai et al. (2005) a similar problem with rather strong initial magnetic field was simulated, and, contrary to our results, the authors did not find the development of MRI. Their simulations of the supernova explosion with weaker magnetic field did not lead to the development of MRI either and hence they did not get supernova explosion for a weak initial magnetic field. The absence of the MRI in their calculations most probably is connected with a rather large numerical viscosity of the numerical scheme they used.

It is known from the observations that the shapes of core collapse supernovae are different. From our simulations it follows that MR supernova explosion arises after development of the MRI. The development of the MRI is a stochastic process and hence the resulting shape of the supernova can vary. We may conclude that MR supernova explosion mechanism can lead to different shape of the supernova. It is important to point out that MR mechanism of supernova explosion leads always to asymmetrical outbursts.

The simulations of the MR supernova explosions are restricted by the symmetry to the equatorial plane. While in reality this symmetry can be violated due to the MRI, simultaneous presence of the initial dipole and quadrupole-like magnetic field, and initial toroidal magnetic field. The violation of the symmetry could lead to the kick effect and formation of rapidly moving radio pulsars.

When rotational and magnetic axes do not coincide the whole picture of the explosion process is three dimensional. Nevertheless, the magnetic field twisting happens always around the rotational axis, so we may expect the kick velocity of the neutron star be strongly correlated with its spin direction, also due to the anisotropy of the neutrino flux. Simultaneously, because of the stochastic nature of MRI, the level of the anisotropy should be strongly variable, leading to a large spreading in the the neutron star velocities.

## 7 CONCLUSIONS

1. In the magnetorotational explosion (MRE) the efficiency of transformation of the rotational energy into the energy of explosion is  $\sim 10\%$ . This is enough for producing core collapse SN from rapidly rotating magnetized neutron star.
2. Development of magneto-rotational instability (MRI) strongly accelerate MRE, at lower values of the initial magnetic fields.
3. The new born neutron star has inside a large (about  $10^{14}$  Gauss) chaotic magnetic field.
4. Jet formation is possible for the dipole-like form of the initial magnetic field, what may have a possible relation to cosmic gamma-ray bursts. Ejection around the equatorial region happens at prevailing of the quadrupole-like component.
5. Braking of the equatorial symmetry, due to initial magnetic field configuration or MRI development, leads to asymmetries in the MRE, and in the neutrino flux, what may explain formation of rapidly moving pulsars and one-side jet formation.

**Acknowledgements** This work was partially supported by RFBR grants 05-02-17697A, 06-02-91157 and 06-02-90864. GSBK is grateful to Franco Giovannelli and other organizers of the workshop for hospitality.

## References

- Akiyama Sh., Wheeler J. C., Meier D. L., Lichtenstadt I., 2003, ApJ, 584, 954  
 Ardeljan N. V., Chernigovskii S. V., 1984, Diff. Uravneniya, 20, 1119  
 Ardeljan N. V., Bisnovaty-Kogan G. S., Kosmachevskii K. V., Moiseenko S. G., 1996, A&AS, 115, 573  
 Ardeljan N. V., Bisnovaty-Kogan G. S., Kosmachevskii K.V., Moiseenko S. G., 2004, Astrophysics, 47, 37  
 Ardeljan N.V., Bisnovaty-Kogan G. S., Moiseenko S. G., 2005, MNRAS, 359, 333  
 Ardeljan N. V., Bisnovaty-Kogan G. S., Popov Yu. P., 1979, Sov. Astron.,23, 705  
 Ardeljan N. V., Bisnovaty-Kogan G. S., Popov Yu. P., Chernigovsky S. V., 1987, Soviet Astronomy, 31, 398  
 Baade W., Zwicky F., 1934, Phys.Rev., 45, 138  
 Bisnovaty-Kogan G. S., 1970, Astron. Zh., 47, 813  
 Bisnovaty-Kogan G. S., 1993, Astron. Ap. Transact., 3, 287  
 Bisnovaty-Kogan G. S., Popov Yu. P., Samokhin A. A., 1976, Ap&SS, 41, 287  
 Bisnovaty-Kogan G. S., Moiseenko S. G., 1992, Astron. Zh., 69, 563  
 Bisnovaty-Kogan G. S., Moiseenko S. G., Ardeljan N. V., 2005, astro-ph/0511173  
 Buras R., Rampp M., Janka H.-Th., Kifonidis K., 2003, Physical Review Letters, 90, 241101

- Burrows A., Hayes J., Fryxell B. A., 1995, ApJ, 450, 830  
Chandrasekhar S., 1981, Hydrodyn. and Hydromag. Stability, NY: Dover  
Colgate S., White R., 1966, ApJ, 143, 626  
Chugai N. N., 1984, Pisma Astron. Zh., 10, 210  
Dessart L., Burrows A., Livne E., Ott C. D., 2006 ApJ, 645, 534  
Hanawa T., Mikami H., Sato Y., Matsumoto T., 2006, AIP Conf. Series, 359, 158  
Iben I. Jr., 1985, Quarterly Journal Royal Astron. Soc., 26, 1  
Imshennik V. S., Nadjozhin D. K., 1972, Zh. Exper. Theor. Phys., 63, 1548  
Ivanova L. N., Imshennik V. S., Nadezhin D. K., 1969, Sci. Inf. of the Astr. Council of the Acad. Sci. USSR., 13, 3  
Janka H.-T., Müller E., 1995, ApJ, 448, L109  
Johnston S., Hobbs G., Vigeland S., Kramer M., Weisberg J. M., Lyne A. G., 2005, MNRAS, 364, 1397  
LeBlanc L. M., Wilson J. R., 1970, ApJ, 161, 541  
Moiseenko S. G., Bisnovatyi-Kogan G. S., Ardeljan N. V., 2006, MNRAS, 370, 501  
O'Connell R., Matese J., 1969, Nature, 222, 649  
Osheroich V. A., Fainberg J., Fisher R. R. et al., 1999, AIP Conference Proceedings, 471, 721  
Sawai H., Kotake K., Yamada S., 2005, astro-ph/0505611  
Spruit H. C., 2002, A&A, 381, 923  
Velikhov E. P., 1959, J. Exper. Theor. Phys., 36, 1398  
Vlemmings W. H. T., Chatterjee S., Briskin W. F. et al., 2005, Memorie della Societa Astronomica Italiana, 76, .531  
Wang J. C. L., Sulkanen M. E., Lovelace R. V. E., 1992, ApJ, 390, 46

## DISCUSSION

**JIM BEALL:** In the dipole jet formation what velocities do you get from the jet, and what is the distribution of these velocities?

**GENNADY BISNOVATYI-KOGAN:** The jet velocities in our calculations are several  $10\,000\text{ km s}^{-1}$ , like in measured SN ejection. We cannot say anything about distribution of these velocities having only few variants of calculations.